JOURNAL OF MATERIALS SCIENCE 18 (1983) 1049–1058

Mechanisms of nucleation and crystallization of lithium disilicate in Li–Zn–silicate glass–ceramic fibres

A. BENEDETTI, G. COCCO, G. FAGHERAZZI*
Istituto di Chimica Fisica, Università Ca' Foscari, DD 2137, 30123 Venezia, Italy

S. MERIANI
Istituto di Chimica Applicata, Università, Via Valerio 2, 34127 Trieste, Italy

G. SCARINCI
Istituto di Chimica Industriale, Università, Via Marzolo 9, 35100 Padova, Italy

The preferred crystal orientation of $Li_2Si_2O_5$ crystallites has been evaluated in several partially crystallized glass fibres with the following chemical composition in mol %: 66.75 SiO_2; 23.45 Li_2O; 8.00 ZnO; 1.00 K_2O and 0.80 P_2O_5. The crystallites were shown to be grown radially with the *c*-axis directed from the surface towards the core of the fibre. When glass fibres have been subjected to a nucleation treatment step, this preferred orientation slightly increases in the temperature range 590 to 620° C, by increasing the crystallinity content. This behaviour was attributed to the presence of active nuclei. A kinetic study on the crystalline volume coarsening, carried out according to the Johnson–Mehl–Avrami equations, showed a mechanism of linear growth for the lithium disilicate phase with the (00*l*) growing planes moved inward from the surface to the core of the fibre. The small-angle X-ray scattering results were obtained by using a masking liquid with an electron density close to that of the glass fibres investigated, in order to eliminate the total external reflection and surface scattering. Results indicated that two distinct particle fractions are precipitated inside the fibres after glass-in glass phase separation and nucleation at 500° C for various periods of time. The fraction of the largest particles, 13 to 20 nm in size, is probably constituted with vitreous SiO_2-rich droplets, whereas the smallest particles, 2.5 to 6.5 nm in size, are probably Li_2O-rich clusters containing P_2O_5.

1. Introduction

In the present paper the results on the preferred crystal orientation shown by $Li_2Si_2O_5$ grown in partially crystallized glass fibres are reported and discussed. The chemical composition (mol %) of the vitreous system analysed is: 66.75 SiO_2, 23.45 Li_2O, 8.00 ZnO, 1.00 K_2O and 0.80 P_2O_5.

As described in the foregoing paper [1], a four-circle diffractometer has been employed to measure the angle, χ, of X-ray intensity distribution along the diffraction cone section. The orientation of the 002 equatorial reflection of $Li_2Si_2O_5$ has been correlated with the crystallinity content of the fibres heated isothermally for various periods of time in the 590 to 620° C temperature range. Furthermore, the $Li_2Si_2O_5$ crystallinity values, obtained with the Hermans and Weidinger method, have been used for a crystallization kinetic study carried out according to the Johnson–Mehl–Avrami (JMA) equations [2–5].

Two crystallization temperatures (590 and 620° C) have been investigated with or without a previous nucleation treatment either at 480 or at

*To whom correspondence should be addressed.

0022–2461/83 $03.00 + .12

TABLE I Angle of distribution of the normals to the (0 0 l) planes of $Li_2Si_2O_5$ crystallites with respect to the fibre external surface, as a function of both the crystallization temperature and time. These values are comprehensive of the mechanical disorientation due to the non-perfect parallelism of the fibres inside the capillary. This disorientation can be considered as a constant added to all $\bar{\eta}$ values indicated. Apart from this systematic error, the relative percentage error can be evaluated as ± 10%

Nucleation treatment	Crystallization temperature (° C)	Angle of distribution of the normals to the (0 0 l) planes of $Li_2Si_2O_5$ for various crystallization times						$\bar{\eta}$
		10 min	20 min	2 h	2.5 h	4 h	10 h	
5 min, 500° C	590	–	–	19.0	–	21.7	–	20.3
5 min, 500° C	610	18.5	17.2	18.1	–	20.8	–	18.6
5 min, 500° C	620	20.0	18.1	17.2	–	16.3	–	17.9
1 h, 480° C	620	–	16.3	–	–	19.0	15.5	16.9
No nucleation	620	–	–	–	19.0	15.5	16.3	16.9

500° C. As a result, the morphological index, n, which depends on the crystal growth mechanism, could be calculated. The X-ray diffraction (XRD) measurements were completed by a careful determination of the edges of the $Li_2Si_2O_5$ orthorhombic unit cell. Finally, in order to cast light on the phase separation mechanism and nucleation, a small angle X-ray scattering (SAXS) study has been undertaken. For this purpose fibres heated isothermally at 480 or at 500° C for various periods of time, were powdered and packed into capillaries 0.5 mm wide, which were filled with a liquid having an electronic density close to that of the glass. As Statton and Hoffman [6] reported, the method allows the elimination of total external reflection and surface scattering.

2. Results on the preferred crystal orientation

Table I shows the angle, η, of distribution of the normals to the (00l) planes of the $Li_2Si_2O_5$ crystallites [1]. Measurements were made on 16

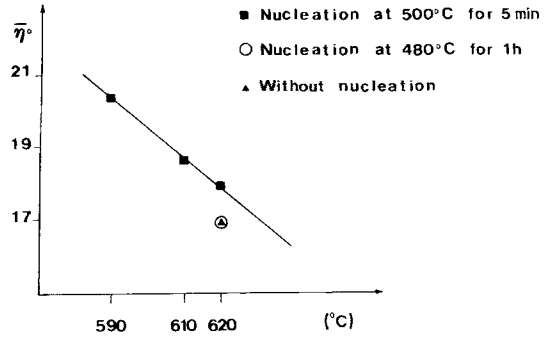

Figure 1 Time averaged, $\bar{n}$, value of distribution angle of the normals to the (0 0 l) planes of $Li_2Si_2O_5$ with respect to the fibre external surface, of the crystallization isotherm.

samples of partially devitrified glass fibres as described in the foregoing paper [1]. The η parameter seems not to depend on heating time.

Only specimens nucleated at 500° C for 5 min and heated at 620° C indicated a systematic slight decrease of η against time. On the other hand, it is possible to see from Fig. 1 that, for a fixed nucleation treatment at 500° C for 5 min, the time averaged value ($\bar{\eta}$) decreases linearly passing from 590 to 620° C. Specimens heated directly at 620° C, or previously nucleated at 480° C for 1 h and then brought to 620° C, showed $\bar{\eta}$ values smaller than those measured for fibres nucleated at 500° C. The first result indicated that the preferred orientation increased by increasing the temperature of crystallization i.e. the crystallinity content, after a fixed nucleation stage was undertaken. The second evidence showed that, for a fixed crystallization temperature, orientation was higher if no nucleation had been carried out or a nucleation stage at 480° C instead of 500° C had been performed. As an illustration of all experimental data, Fig. 2 shows the relative X-ray intensity against χ curves, obtained for the specimens heated at 520° C for 10 min or for 2 h respectively, after a 5 min nucleation step at 500° C. The two parallel lines represent the background counts.

The former of the two above cited results is apparently in disagreement with the trend observed by Booth and Rindone [7] for Li_2O–2.75 mol% SiO_2 glass–ceramic fibres which were directly treated at high temperatures, from 550 up to 800° C, without a previous treatment. In this last case the observed increase in crystallinity content was accompanied by a decrease in preferred orientation. This fact could be attributed to the rapid formation of crystals by homogeneous

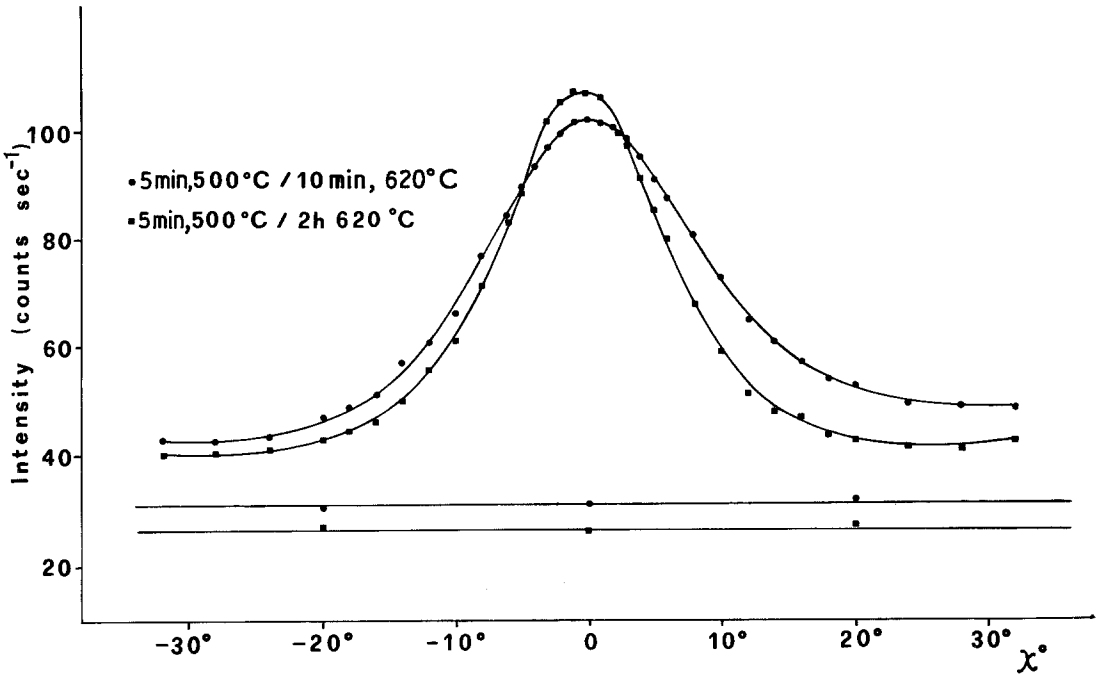

Figure 2 X-ray relative intensity against χ plots for two glass–ceramic fibre specimens with a different degree of orientation.

nucleation within the fibre mass. In the present case, in contrast , the observed behaviour can be ascribed to the initial presence of active nuclei which were formed during the first heating stage at 500° C.

3. Kinetics for $Li_2Si_2O_5$ crystallization

In Fig. 3 the crystal volume fraction or crystallinity, C, of the four series of specimens shown in Table I of the foregoing paper [1] are plotted as a function of time. From Fig. 3 it is possible to see that the nucleation at 500° C for 5 min was much more effective than the nucleation at 480° C for 1 h, with respect to the crystallization rate subsequently carried out at 620° C. This is in good agreement with the investigation of various authors [8–10] who found, especially by transmission electron microscopy (TEM), that the maximum nucleation rate in Li_2O–SiO_2–ZnO–P_2O_5–K_2O mass glassy systems was placed at about 500° C. In these latter systems the ZnO content was lower than the present one (1 to 3 instead of 8 mol%), whereas the molar ratio SiO_2/Li_2O was in the range 2.3 to 3.3 to be compared with the present value of 2.85. The amounts of K_2O and P_2O_5 were close to the values employed here.

With regard to the kinetic behaviour of the fibres heated directly at 620° C, without a nucleation pre-treatment, Fig. 3 shows the presence of an incubation time of about 30 min for crystal coarsening to begin. The kinetics displayed by the curves in Fig. 3 can be theoretically explained on the basis of the well known JMA equation [2–5]:

$$V = 1 - \exp(-kt^n) \quad (1)$$

where V is the volume fraction of the crystalline phase; it was calculated from the crystallinity, C, values reported in the foregoing paper [1] taking into account suitable normalization conditions; n is a morphological index which depends theoretically on the assumed model of crystal growth; k is a constant related to the absolute temperature, T, by an Arrhenius – type equation:

$$k \propto \exp(-E/RT) \quad (2)$$

where E is the activation energy for volume crystallization and R is the gas constant.

Assuming that at $t = 0$ the glass contains randomly distributed active nuclei and that more nuclei are not formed during crystal coarsening, as occurs when a glass has been subjected to a sufficiently effective nucleation stage and the

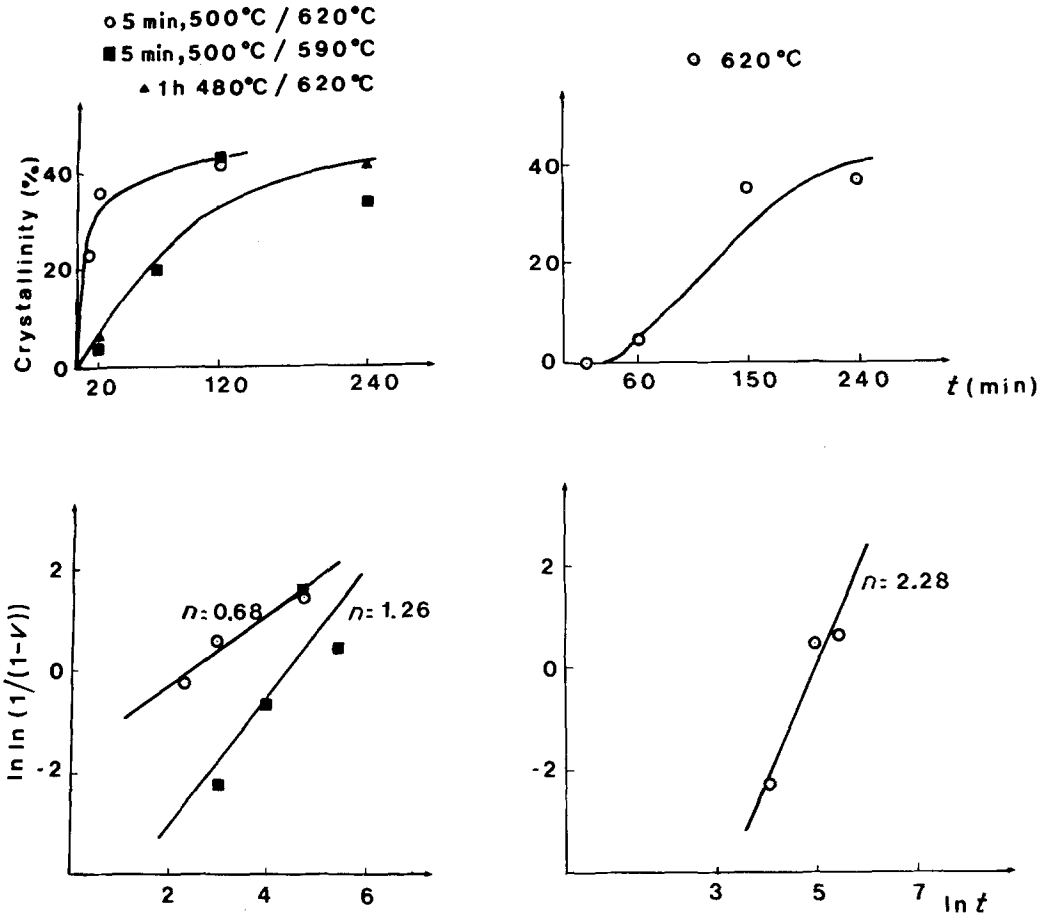

Figure 3 Kinetic curves for the Li_2Si_2O crystallization at 590 or at 620° C with or without a previous nucleation stage at 480 or at 500° C.

crystallization temperature is well above the temperatures of high nucleation rates, a value of $n = 1$ corresponds to rod-like linear growth, a value of 2 corresponds with two-dimensional plate-like growth and a value of 3 to three-dimensional bulk growth. When, in contrast, nucleation and crystallization occur simultaneously in one single stage, then the n exponent in Equation 1 must be raised by one unit for each of the three above mentioned crystal growth mechanisms [11, 12].

TABLE II The Avrami's exponent (or morphological index), n, and the logarithm of the rate constant, k, for the three crystallization isotherms studied

Crystallization isotherm	Avrami's Exponent, n	$\ln k$
(5 min, 500° C) 590° C	1.26	− 5.7
(5 min, 500° C) 620° C	0.68	− 1.7
(No nucleation) 620° C	2.28	−11.5

Following the Avrami concept, we have plotted in Fig. 3 the $\ln \ln (1/(1 - V))$ against $\ln t$, obtaining in this way the n and $\ln k$ values indicated in Table II. For the crystallization at 590 and at 620° C, following a nucleation step at 500° C, n is not too far from 1, whereas, for a direct crystallization at 620° C it is close to 2. These results agree well with the previous theory and strongly support the above proposed model which consists in a crystallization of rod-like crystals of $Li_2Si_2O_5$ grown radially from the external surface to the fibre core. As indicated by Hench *et al.* [13] for cases when nucleation treatment is insufficient, as might be when, in the present case, nucleation was made at 480° C for 1 h, the incubation time for the crystallization process may remain constant although fewer sites could

TABLE III Interplanar distances d_{130}, d_{040}, d_{002}, d_{111} and unit cell edges a, b, c, of the orthorhombic lattice of $Li_2Si_2O_5$ grown in partially crystallized glass fibres subjected to various heating cycles. The error could be evaluated as ± 0.0003 nm

Heat treatment	d_{130} (nm)	d_{040} (nm)	d_{002} (nm)	d_{111} (nm)		a(nm)	b(nm)	c(nm)
				observed	calculated			
(5 min, 500° C) 10 min, 620° C	0.3748	0.3660	0.2405	0.3603	0.3601	0.585	1.464	0.481
(5 min, 500° C) 20 min, 620° C	0.3743	0.3648	0.2402	0.3599	0.3599	0.586	1.459	0.480
(5 min, 500° C) 2 h, 620° C	0.3729	0.3638	0.2396	0.3584	0.3587	0.583	1.455	0.479
(5 min, 500° C) 4 h, 620° C	0.3712	0.3620	0.2390	0.3570	0.3577	0.581	1.448	0.478
Li_2SiO_5 [13]	0.375	0.367	0.2395	–	0.359	0.580	1.466	0.4806

reach critical size. As a result, the crystallization rate becomes slower. A comparison between the two C against t curves displayed in Fig. 3, for isothermal crystallization at 620° C, just indicates that nucleation at 480° C for 1 h was much less effective than the nucleation at 500° C for only 5 min.

A determination of the edges a, b and c of the orthorhombic unit cell of lithium disilicate has been performed employing a powder diffractometer at suitable experimental conditions (reflection technique, Cu$K\alpha$ radiation, scan of 0.25° min^{-1}, calibration with Si standard). Table III shows the d_{130}, d_{040} and d_{002} interplanar distances obtained for all the specimens crystallized at 620° C after a nucleation stage at 500° C for 5 min. From these three independent experimental values a, b and c have been deduced. The two last columns of Table III show both the d_{111} observed and calculated values which show a good agreement.

The systematic decrease of a, b and c by increasing the heating time is quite evident within this series of specimens. This trend was only qualitatively observed for the other specimens subjected to different heating cycles. Other possible X-ray diffraction lines were too weak to be considered with reliable accuracy. From these results it can be deduced that, at the beginning of crystallization, the unit cell edges are closer to those reported by Donnay and Donnay [14] for pure $Li_2Si_2O_5$ than the corresponding values measured at the end of the isothermal heating stage (4 h at 620° C). This behaviour can be explained on the basis of a possible formation of a solid solution very rich in $Li_2Si_2O_5$ whose evolution could be associated with the formation of Li_2ZnSiO_4, as reported in the foregoing paper [1]. No relevant line broadening was observed for all the specimens analysed. This shows that the coarsening of the nucleated crystals should be very fast at the temperatures investigated here.

4. Glass-in glass phase separation and nucleation

A SAXS study was undertaken on several samples of glass fibres heated at 500° C within a 1 min to 10 h range in order to evaluate the sub-microscopic heterogeneities due to glass-in glass separation and nucleation. This temperature was chosen on the basis of literature data [8–10] reported on mass glassy systems of similar composition, as well as on the basis of the previously described kinetic studies on the crystallization of lithium disilicate.

As indicated by Statton and Hoffmann [6] as well as by Cartz [15], the total external reflection and surface scattering presented by the glass fibres strongly bias or completely hide the SAXS signal due to the presence of internal heterogeneities. Therefore, we have attempted to overcome this difficulty by placing the powdered heat treated fibres into 0.5 wide capillaries, filled with a liquid having an electron density slightly higher than that of the glassy material (the liquid employed was CH_2I_2 with an electron density of 1.37 g electron cm^{-3} to be compared with that of 1.23 g electron cm^{-3} pertaining to the present vitreous system, its mass density being 2.5 g cm^{-3}; on the other hand, the electron density of vitreous silica is 1.09 g electron cm^{-3}).

SAXS measurements were carried out according to "infinite primary beam" conditions with Kratky-PAAR camera equipped with an electronic step scanner. Zirconium-filtered Mo$K\alpha$ radiation

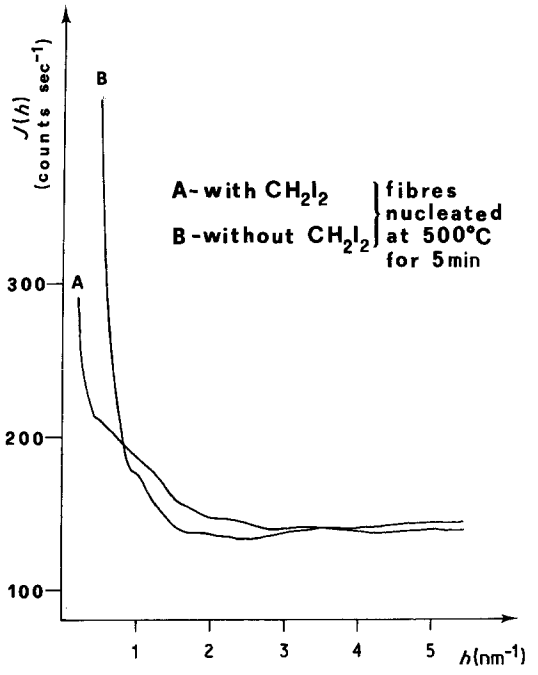

Figure 4 SAXS curves corresponding to the glass fibres nucleated at 500° C for 5 min either immersed in the masking liquid (A) or not (B).

and a scintillation detector with pulse height analyser were employed. The SAXS intensities, J, averaged on three runs, each of 4×10^4 fixed counts, were normalized to equal X-ray optical density and equal relative primary beam intensity. The parasitic scattering was negligible. It is worth noting that all capillaries containing CH_2I_2 gave similar optical density values since the powdered fibres were packed to similar apparent densities.

Fig. 4 shows two J against h curves corresponding to the glass-fibres nucleated at 500° C for 5 min, either immersed into the masking liquid (A) or not (B), where $h = 4\pi (\sin\theta)/\lambda$, where 2θ is the Bragg angle and λ is the wavelength. Due to the total external as well as to the surface scattering, the SAXS curve for the material not immersed in CH_2I_2 is anomalously high for 2θ angular values shorter than about 30 minutes of arc. This angular range agrees well with those indicated or calculated by the previously cited authors [6–15], for these two causes of X-ray scattering at very low angles. In contrast, when the masking liquid is used, this scattering drastically diminishes, whereas the scattering due to the internal micro-heterogeneities is better displayed.

From Fig. 5 it is possible to compare the J against h curves of the "as-quenched" fibres, immersed in CH_2I_2, with a glass platelet having the same chemical composition and a thickness of 0.55 mm (optical density = 1.25). The curve of the specimen nucleated at 500° C for 10 h is also shown in Fig. 5. Similar Guinier diameters were obtained for both the "as-quenched" glass fibres (18.2 nm) and the "as-quenched" glass platelet (15.0 nm). The trend of the SAXS curve of this latter sample, which was suitably polished in order to avoid surface scattering [16] is not too far from the one due to the initial glass fibres first powdered and then immersed into capillaries

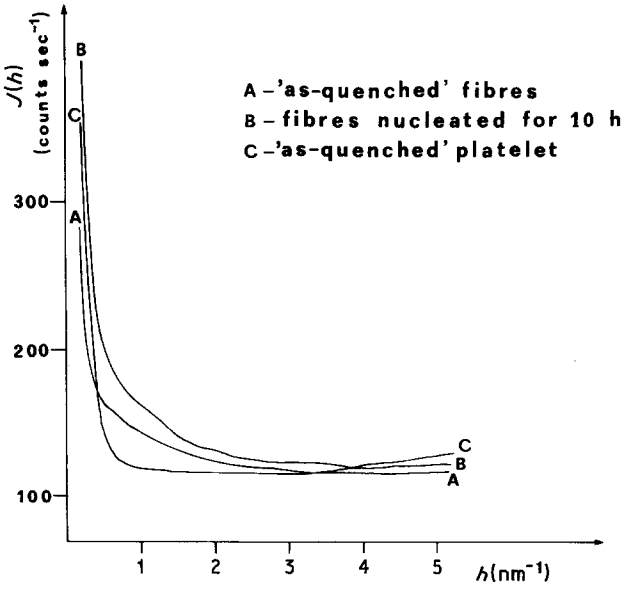

Figure 5 SAXS curves corresponding to the "as-quenched" glass fibres (A), to the same fibres nucleated for 10 h (B) and to an "as-quenched" glass platelet having the same composition of that of the glass fibres (C).

TABLE IV Guinier diameters calculated for spherically-shaped particles (SiO_2-rich or Li_2O-rich)

Specimen treatment	D_G(nm)		Q_0 (arbitrary units)
	Large particles (SiO_2rich)	Small particles (Li_2O-rich)	
As-quenched fibre	18.2	–	5.3
1 h, 480° C	18.6	2.6	5.9
1 min, 500° C	17.6	–	7.8
5 min, 500° C	13.8	3.2	10.1
1 h, 500° C	13.0	3.2	7.9
10 h, 500° C	17.2	5.6	9.4
1 h, 500° C and 20 min, 570° C	12.8	6.2	7.0
As-quenched glass-platelet	15.0	–	4.5

filled with CH_2I_2. All these results well support the validity of the masking liquid method.

After having established in this way, the reliability of the method, we have investigated two other specimens nucleated at 500° C for 1 min and 1 h respectively, a specimen nucleated at 500° C for 1 h and subsequently heated at 570°C for 20 min, in order to attempt to coarsen the preformed nuclei and, finally, a specimen nucleated at 480° C for 1 h. Except for the initial fibres and those nucleated only for 1 min, all other samples clearly show two distinct slopes in the Guinier $\log_{10} J$ against h^2 plots, corresponding to two distinct, D_G diameters. These parameters, which have been calculated for spherically shaped particles according to known equations [17], are given in Table IV. The Guinier particle diameter is defined in terms of the square root of the ratio of the seventh to the fifth moment of the size distribution of the particles [18, 19].

As an illustration of the Guinier plots, Fig. 6 shows the $\log_{10} J$ against h^2 curves of two fibre specimens. For these specimens Fig. 7 displays the related Porod plots: Jh^3 against h, from which a double plateau of maximum indicates a bimodal size distribution [26]. In all these plots, as well as in the following calculation of the invariant, the background due to the matrix scattering was suitably subtracted from the J intensities according to the Luzzati procedure [21], extensively applied by various authors in many different systems [16, 22, 23].

The high angle asymptotic $Jh^3 = \text{constant}$ behaviour is not followed during the early stages of amorphous phase separation and nucleation owing to the absence of a sharp interface between the separated particles and matrix. For this reason the invariant or integrated intensity, Q_0, defined by

$$Q_0 = \text{constant} \int_0^\infty hJ(h)\, dh \qquad (3)$$

may be affected by systematic errors.

In order to cast light on the nature of the amorphous phase separation and nucleation, the Q_0 parameter for all samples, has been calculated in relative units employing exactly the same criteria for determining the Porod constant beyond the second plateau in the Jh^3 against h curve. As a result, the curve shown in Fig. 8 was obtained for Q_0 as function of the logarithm of time for the nucleation at 500° C. Also in Fig. 8 D_G is plotted for both particle fractions. The relative error for Q_0 may be estimated as ± 15 %.

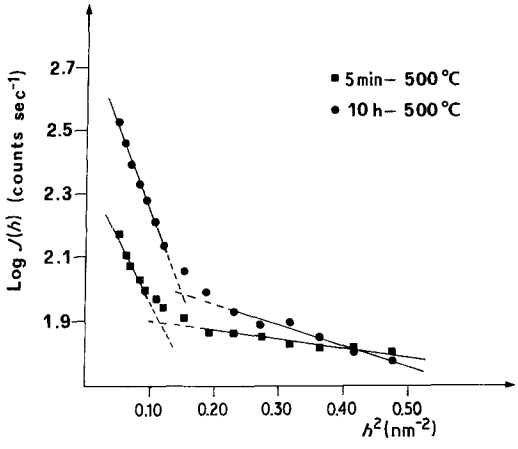

Figure 6 Guinier plots: $\log_{10} J$ against h^2, for two fibre specimens nucleated at 500° C for 5 min and for 10 h.

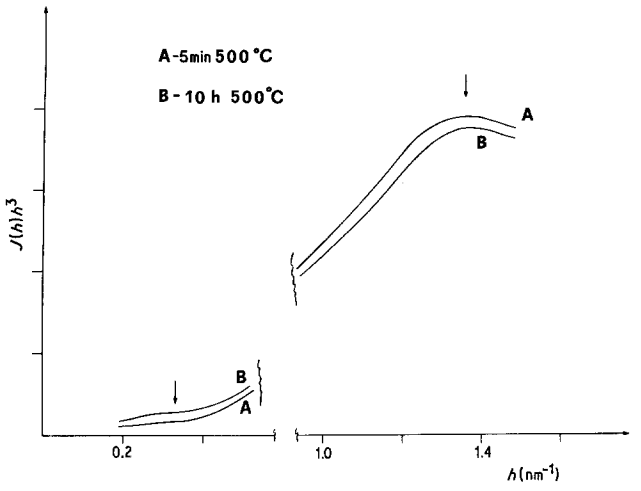

Figure 7 Porod plots: Jh^3 against h, for two fibre specimens nucleated at 500° C for 5 min and for 10 h.

Bearing in mind the literature data obtained by SAXS as well as by TEM and other techniques on glass-in glass separation and nucleation in bulky glasses of both Li_2O–SiO_2 [13, 24–32] and Li_2O–ZnO–SiO_2 [8–10, 33–34] systems, it is possible to explain the present SAXS results (which unfortunately cannot be supported here by any TEM replica micrographs owing to the impossibility of obtaining suitable fracture surfaces) as follows. Initially, within the "as-quenched" fibres SiO_2-rich glass droplets with a diameter of about 18.0 nm, are segregated. These particles probably do not reach, at 500° C, the coarsening stage.

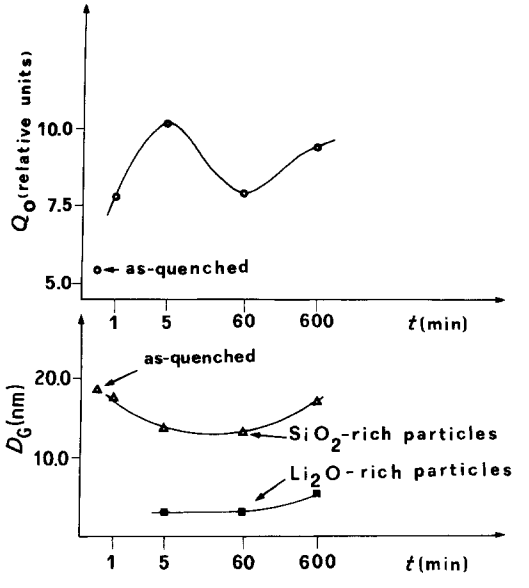

Figure 8 Plots of Q_0 integrated intensity (in relative units) and Guinier diameters, against time, for the fibre specimens nucleated at 500° C.

James and McMillan [25] showed the presence of dispersed particles with a composition rich in silica in an "as-quenched" glass the composition of which was (mol%) 69 SiO_2, 30 Li_2O and 1 P_2O_5. The low electron density of this separated phase, compared with the matrix electron density can well justify the SAXS signal if one takes into account the basic relation [35]

$$Q_0 \propto V_p (\rho - \rho_0)^2, \qquad (4)$$

where V_p is the total volume of the scattering particles and $(\rho - \rho_0)$ is the electron density difference between the particles and matrix. As shown by some authors, the V_p occupied by the separated silica-rich phase could be relatively high [25, 26].

Subsequently, small nuclei appear, whose sizes slightly increase with time (see Fig. 8), as the nucleation stage at 500° C goes on. This is in agreement with the results of Hing and McMillan [9] who established the influence of phosphorus pentoxide in promoting internal nucleation in Li_2O–SiO_2 as well as in Li_2O–ZnO–SiO_2 glasses at 500° C. Some fine structure appeared between the phase-separated droplets, the nature of which was not possible to elucidate. In addition, they noted that in the Li_2O–ZnO–SiO_2 system containing K_2O, as in the present one, the mean size of the SiO_2-rich droplets was much smaller than in the corresponding glass not containing K_2O.

The trend of the Q_0 against ln t curve, shown in Fig. 8, displays a maximum of about 5 min. This agrees with the interpretation that transient nuclei precipitate inside the glass fibres, which progressively change their chemical composition or become completely resorbed by the matrix

as the equilibrium lithium disilicate crystalline nuclei appear. The precursor nuclei are probably originated on P_2O_5 molecular groups, as suggested by James and McMillan [25] and Harper and McMillan [26], who indicated the presence of clusters of composition 3 $Li_2O{\cdot}P_2O_5$ in the Li_2O-rich phase. Then it is highly probable that the $Li_2Si_2O_5$ crystals nuclei grow on the surfaces of these associated compounds.

The SAXS signal, actually due to these Li_2O-rich clusters, which have a significant lower electron density than that of the matrix rich in zinc, is added to the signal due to the phase separated silica-rich droplets since interference effects between the two different dilute particle populations is highly unlikely. Therefore Q_0 is maximized when the contribution to $(\rho - \rho_0)^2$, given by the Li_2O-rich particles, is very high owing to the maximum difference in composition between the clusters and matrix. Afterwards, when the composition of these precursor nuclei approaches that of the crystalline lithium disilicate, a decrease in electron density difference occurs. The latter is subsequently balanced by an increase in the total volume occupied by the nucleated phase, as the time of the isothermal heating has increased (see Fig. 8 and Equation 4). It is worth noting that some authors have also hypothesized a transient formation of lithium metasilicate in Li_2O–SiO_2 or in Li_2O–ZnO–SiO_2 systems, both nucleated at 500° C for times ranging from one to several hours [8, 13]. On the other hand, James and McMillan [25] observed a fast kinetics of nucleation, of the order of minutes, at 550° C of heat treatment in a Li_2O–SiO_2 glass containing 1 mol% of P_2O_5.
1 mol% of P_2O_5.

The fact that the nucleation at 500° C for 5 min was shown to be more active for the subsequent crystal coarsening at higher temperatures than the nucleation at 480° C for 1 h, as displayed by the foregoing kinetic studies, is in agreement with the present SAXS results (see the respective Q_0 values given in Table IV). The concurrent presence of amorphous phase separation and nucleation suggests a possible relationship between the two phenomena, as was very recently reported by Zanotto and Craievich [36] who substantially confirmed a previous work of Tomozawa [28].

Moreover, we observe that, in the present glass system, spinodal decomposition is very unlikely since the composition, as referred to the Li_2O/SiO_2 molar ratio, is far from the centre of the immiscibility gap [28, 36–37] of the related binary system.

Lastly, we must not forget that, besides the present mechanism of internal nucleation, the fibre surface also certainly plays an important role in triggering the nucleation and the oriented crystallization process which starts from the Li_2O-rich particles situated in the outer rim, close to the surface, as Booth and Rindone [17] have already indicated.

5. Conclusions

This paper reports the results obtained concerning the preferred crystal orientation and the kinetics of the crystallization process of $Li_2Si_2O_5$ in Li_2–ZnO–SiO_2 glass–ceramic fibres containing K_2O and P_2O_5 as minor phases. The orientation of $Li_2Si_2O_5$ was shown to cause a radial growth of crystallites with their c-axis preferentially pointed from the external surface towards the centre of the circular fibre section. In the temperature range from 590 to 620° C the orientation increases when crystallinity content increases, after a fixed nucleation step has been carried out. This behaviour was attributed to the presence of active nuclei.

As explained by Booth and Rindone [7] the (002) plane is the richest one in lithium, inside the lithium disilicate unit cell. The growth of this plane starting from Li_2O-rich particles, parallel to the surface, would then account for the observed orientation.

According to Libeau [38] lithium disilicate has a chain structure parallel to c-axis and therefore it is possible to conclude that the chains are preferentially observed to grow perpendicularly to the fibre axis.

A kinetic study on the crystalline volume coarsening, carried out according to the JMA equation showed a linear growth mechanism for the lithium disilicate phase with the (00l) growing planes which move inward from the surface to the core of the fibre. The role played by the nucleation treatment on the crystallization mechanism has been clarified by computing the morphological index, n from the kinetic curves and observing the presence of an incubation time when the nucleation step did not occur. From a X-ray peak angular position study a slight narrowing of the orthorhombic lithium disilicate unit cell was observed for long crystallization times. This can be attributed to a lithium disilicate-rich

solid solution formation in concurrence with the appearance of very weak lines due to the lithium–zinc–silicate crystalline phase.

The SAXS results indicated that two distinct particle fractions are precipitated inside the fibres after glass-in glass phase separation and nucleation occurred at 500° C for various periods of time.

The fraction of the largest particles, 13.0 to 20.0 nm in size, is probably constituted by vitreous SiO_2-rich droplets, whereas the smallest particles, 2.5 to 6.5 nm in size, are probably Li_2O-rich clusters containing P_2O_5. The integrated intensity analysis showed the formation, at short times of the order of minutes, of precursor nuclei which subsequently reach the lithium disilicate composition.

Acknowledgements

We thank the Italian Research Council (CNR, Rome) for the financial support obtained for this work in the "Progetto Finalizzato Chimica Fine e Secondaria – Sottoprogetto Metodologie" research programme. The assistance of Mr F. Venuda in the experimental work is gratefully acknowledged.

The four-circle diffractometer was kindly placed at our disposal for the preferred orientation measurements by Professor D. Clemente of Istituto di Chimica e Tecnologia dei Radioelementi (CNR, Padova, Italy).

References

1. A. BENEDETTI, G. COCCO, G. FAGHERAZZI, R. LOCARDI and S. MERIANI, *J. Mater Sci.* **18** (1983) 1039.
2. M. AVRAMI, *J. Chem. Phys.* 7 (1939) 1103.
3. *Idem, ibid.* 8 (1940) 212.
4. *Idem, ibid.* 9 (1941) 177.
5. R. F. MEHL, "The Physics of Hardenability" (Syposium on Hardenability, American Society of Metals, Detroit, October, 1938).
6. O. STATTON and L. C. HOFFMAN, *J. Appl. Phys.* **31** (1960) 404.
7. C. L. BOOTH and G. E. RINDONE, *J. Amer. Ceram. Soc.* 47 (1964) 26.
8. P. W. McMILLAN, S. V. PHILLIPS and G. PARTRIDGE, *J. Mater. Sci.* **1** (1966) 269.
9. P. HING and P. A. McMILLAN, *ibid.* 8 (1973) 340.
10. G. PARTRIDGE, *Glass Technol.* **20** (1979) 246.
11. S. W. FREIMAN and I. L. HENCH, *J. Amer. Ceram. Soc.* **51** (1968) 382.
12. P. HANTOJÄRVI, A. VEHANEN, V. KOMPA and E. POJANNE, *J. Non-Cryst. Solids* **29** (1978) 365.
13. L. L. HENCH, S. W. FREIMAN and D. L. KINSER, *Phys. Chem. Glasses* **12** (1971) 58.
14. G. DONNAY and J. D. H. DONNAY, Amer. Mineral. **38** (1953) 163.
15. L. CARTZ, *J. Appl. Phys.* **68** (1964) 2274.
16. J. A. WILLIAMS, G. E. RINDONE and H. A. McKINSTRY, *Amer. Ceram. Soc.* **64** (1981) 697.
17. A. GUINIER and G. FOURNET, "Small-Angle Scattering of X-rays" (John Wiley and Sons, New York, 1955) p. 126.
18. S. D. HARKNESS, R. W. GOULD and J. J. HREN, *Phil. Mag.* **19** (1969) 157.
19. R. BAUER and V. K. GEROLD, *Acta Metall.* **12** (1969) 1449.
20. G. F. NEILSON, *Discuss. Faraday Soc.* **50** (1979) 145.
21. V. LUZZATI, J. WITZ and A. NICOLAIEFF, *J. Mol. Biol.* 3 (1961) 379.
22. W. RULAND, *J. Appl. Cryst.* 4 (1971) 70.
23. C. G. VONK, *ibid.* 9 (1976) 433.
24. K. NAKAGAWA and T. IZUMITANI, *Phys. Chem. Glasses* **10** (1969) 179.
25. P. F. JAMES and P. W. McMILLAN, *ibid.* **11** (1970) 64.
26. H. HARPER and P. W. McMILLAN, *ibid.* **13** (1972) 97.
27. R. H. DOREMUS and A. M. TURKALO, *ibid.* **13** (1972) 14.
28. M. TOMOZAWA, *ibid.* **13** (1972) 161.
29. K. MATUSITA and M. TASHIRO, *ibid.* **14** (1973) 77.
30. K. MATUSITA, T. MAKI and M. TASHIRO, *ibid.* **15** (1974) 106.
31. P. F. JAMES, *ibid.* **15** (1974) 95.
32. M. TASHIRO, in "Proceedings of the 8th International Congress on Glass" (Society of Glass Technology, Sheffield, 1968) p. 113.
33. G. PARTRIDGE, S. V. PHILLIPS and J. N. RILEY, *Trans. J. Brit. Ceram. Soc.* **72** (1973) 255.
34. P. VINCENZINI and B. MARCHESE, *Ceramurgia* **4** (1974) 91.
35. A. GUINIER, "X-ray diffraction" (W. H. Freeman, San Francisco, 1963) p. 338.
36. E. D. ZANOTTO and A. F. CRAIEVICH, *J. Mater. Sci.* **16** (1981) 973.
37. R. J. CHARLES, *J. Amer. Ceram. Soc.* **50** (1967) 631.
38. F. LIEBAU, *Acta Cryst.* **14** (1961) 389.

Received 26 May
and accepted 31 August 1982